



Mechanical forces regulate the reactivity of a thioester bond in a bacterial adhesin

Received for publication, January 18, 2017, and in revised form, March 17, 2017. Published, Papers in Press, March 27, 2017, DOI 10.1074/jbc.M117.777466

Daniel J. Echelman¹, Alex Q. Lee, and Julio M. Fernández

From the Department of Biological Sciences, Columbia University, New York, New York 10027

Edited by Chris Whitfield

Bacteria must withstand large mechanical shear forces when adhering to and colonizing hosts. Recent structural studies on a class of Gram-positive bacterial adhesins have revealed an intramolecular Cys-Gln thioester bond that can react with surface-associated ligands to covalently anchor to host surfaces. Two other examples of such internal thioester bonds occur in certain anti-proteases and in the immune complement system, both of which react with the ligand only after the thioester bond is exposed by a proteolytic cleavage. We hypothesized that mechanical forces in bacterial adhesion could regulate thioester reactivity to ligand analogously to such proteolytic gating. Studying the pilus tip adhesin Spy0125 of *Streptococcus pyogenes*, we developed a single molecule assay to unambiguously resolve the state of the thioester bond. We found that when Spy0125 was in a folded state, its thioester bond could be cleaved with the small-molecule nucleophiles methylamine and histamine, but when Spy0125 was mechanically unfolded and subjected to forces of 50–350 piconewtons, thioester cleavage was no longer observed. For folded Spy0125 without mechanical force exposure, thioester cleavage was in equilibrium with spontaneous thioester reformation, which occurred with a half-life of several minutes. Functionally, this equilibrium reactivity allows thioester-containing adhesins to sample potential substrates without irreversible cleavage and inactivation. We propose that such reversible thioester reactivity would circumvent potential soluble inhibitors, such as histamine released at sites of inflammation, and allow the bacterial adhesin to selectively associate with surface-bound ligands.

Thioester bonds are ubiquitous in biology and are commonly employed as reactive intermediates in metabolic pathways, including ubiquitinylation (1), fatty acid synthesis (2), and non-ribosomal peptide synthesis (3). In addition, there are two rare but notable examples of intramolecular thioester bonds that

form between Cys and Gln/Glu side chains: in the $\alpha 2$ -macroglobulin (A2M)² anti-proteases and in the C3 and C4 proteins of the immune complement system (4–6). In both cases, the thioester bond functions as the electrophilic substrate to draw a nucleophilic ligand and create an intermolecular covalent bond with the target (7). Moreover, both A2Ms and the immune complement proteins utilize a proteolytic gating mechanism to regulate thioester reactivity; the thioester bond is protected and buried in the hydrophobic core until a specific proteolytic cleavage un masks the bond to react with local nucleophiles (7). For example, the A2M anti-protease acts through a “Venus fly-trap mechanism” whereby a bait region of A2M attracts a protease that subsequently cleaves A2M, exposing the thioester to irreversibly react with and inactivate the protease (4, 6). For C3, proteolysis occurs at target surfaces by upstream effectors of the immune complement pathway. Once cleaved, C3 readily reacts with ligands on the microbial cell with a half-life of microseconds (5, 8).

A third class of intramolecular thioester bonds was recently discovered among extracellular adhesins of Gram-positive bacteria (9–11). These thioester domains (TEDs) are distributed broadly across six bacterial genera and share a conserved α/β -fold despite generally low sequence homology (as low as 12% pairwise identity between TEDs with solved crystal structures) (11). Analogous to C3 and C4, which covalently bind to microbial surfaces via the thioester, bacterial TEDs have appropriated the thioester mechanism to bind to host targets. To date, one physiological ligand, fibrinogen, has been identified as a substrate of two bacterial TEDs, which react via their Cys-Gln thioester bond with a specific lysine side chain in fibrinogen (11). However, unlike the prototypical mechanisms of A2M, C3, and C4, no proteolytic activation is needed.

We hypothesized that mechanical unfolding, rather than proteolysis, could modulate thioester reactivity in the bacterial TED. Physiological forces are known to unfold proteins, including the titin of muscle (12), the adhesive pili of Gram-negative bacteria (13), and the spectrin of the cytoskeleton (14). Moreover, mechanical unfolding exposes buried residues to chemical modification (14, 15). Bacterial adhesins can experience extreme physiological shearing forces, and certain Gram-positive adhesins are correspondingly adapted to remain folded up to ~ 700 pN, the highest forces reported for protein mechanical stability (16). Could mechanical force also fine-tune the reactivity of the thioester bond in bacterial adhesins?

This work was supported in part by National Institutes of Health Grants GM116122 and HL061228 (to J. M. F.). The authors declare that they have no conflicts of interest with the contents of this article. The content is solely the responsibility of the authors and does not necessarily represent the official views of the National Institutes of Health.

This article was selected as one of our Editors' Picks.

This article contains supplemental Figs. S1–S6, Tables S1–S2, Methods, and Refs. 1–15.

¹ Supported by a National Institutes of Health Medical Scientist Training Program Grant to Columbia University. To whom correspondence should be addressed: Dept. of Biological Sciences, Columbia University, 550 West 120th St., New York, NY 10027. Tel.: 212-854-9474; E-mail: dje2122@columbia.edu.

² The abbreviations used are: A2M, $\alpha 2$ -macroglobulin; pN, piconewton; AFM, atomic force microscopy; PDB, Protein Data Bank; TED, thioester domain.

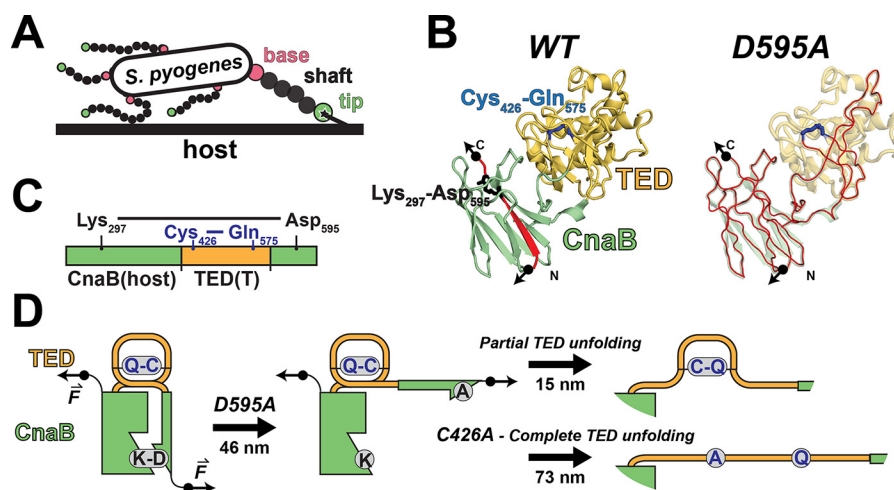


Figure 1. Structure and mechanics of *S. pyogenes* pilus adhesion. *A*, schematic representation of a Gram-positive bacterium adhering to host via its pilus, which is composed of base, shaft, and tip pilin subunits. *B*, truncated structure of the Spy0125 tip adhesin used in this study, composed of a CnaB Ig-type domain with an internal isopeptide bond (Lys-Asp, shown in black) and a thioester domain (TED) with an internal thioester bond (Cys-Gln, shown in blue; PDB code 2xid (11)). The thioester domain is inserted within the fold of CnaB. Predicted pathways for axial force transduction for the wild-type and isopeptide mutant (D595A) are traced in red. Schematic representations of the linear sequence (*C*) and the contact map (*D*) for CnaB-TED, showing the mechanical unfolding pathway with sequential mutations to remove the Lys-Asp (K-D) isopeptide bond (D595A mutation) and the Cys-Gln (C-Q) thioester bond (C426A mutation). Predicted contour length increments upon unfolding are indicated.

Here, we developed a single-molecule technique to study thioester chemistry with atomic force microscopy (AFM)-based force spectroscopy. Using the Spy0125 pilus adhesin from *Streptococcus pyogenes* as our model bacterial TED, we unambiguously identify the state of the thioester bond (formed versus cleaved) with chemical and mutagenic modifications. We find that methylamine and histamine nucleophiles can cleave the thioester bond in the folded Spy0125. Critically, the Cys-Gln thioester bond spontaneously reforms at zero-force, preventing such soluble nucleophiles from permanently inactivating the adhesin. Finally, we propose that the Gram-positive bacterial TED may bind ligands in a reversible regime at zero-force, but with a longer-lived interaction at sufficiently high force.

Results

CnaB mechanically protects its inserted thioester domain

Intramolecular covalent bonds are abundant in Gram-positive surface proteins, which include common disulfide bonds in addition to more unique Lys-Asn/Asp isopeptide bonds, Thr-Gln ester bonds, and Cys-Gln thioester bonds (17, 18). These internal covalent bonds have a pronounced effect on the mechanical properties of their proteins, often increasing stability, accelerating folding, and delimiting extensibility (16, 19).

We predicted that the thioester bond would delimit extension in a model bacterial TED, Spy0125, from the Gram-positive *S. pyogenes*. Spy0125 covalently cross-links at the tip of the Spy0128-type pilus, a fibrous adhesive appendage composed of isopeptide-bonded Spy0128 repeats along its shaft and linked by an isopeptide bond to the cell wall at its base, resulting in a fully covalent megadalton-scale structure (Fig. 1A) (20).

The Spy0125 adhesin is a four-domain protein, composed of two structural Ig-type CnaB domains with internal Lys-Asn/Asp isopeptide bonds and two TEDs (TED(N) and TED(T)) with internal Cys-Gln thioester bonds (supplemental Fig. S1A) (10). Uniquely, TED(T) is inserted in the fold of a host CnaB

(Fig. 1, B and C). Some strains of *S. pyogenes* express Spy0125 without the N-terminal TED, TED(N) (9), and deletion of the N-terminal TED alone has no appreciable effect on adhesion (20). As a result, we chose to focus our study of thioester reactivity on the inserted TED(T) in its host CnaB, hereafter referred to as CnaB-TED. Using AFM-based single-molecule force spectroscopy, we previously demonstrated that CnaB-type domains are mechanically inextensible because of the intramolecular Lys-Asn/Asp isopeptide bond (21). Indeed, we find that the host CnaB is mechanically inextensible when the Lys-297–Asp-595 isopeptide bond is present (supplemental Fig. S1, C and D). In turn, no unfolding of the inserted TED is observed while the CnaB isopeptide bond is present. We therefore removed the CnaB isopeptide bond to study thioester reactivity in an AFM-based single molecule assay. We engineered a polyprotein having four tandem repeats of the host-insert CnaB-TED pair with a D595A isopeptide mutation, hereafter referred to as poly-CnaB_{D595A} TED. We further appended two cysteine residues to the C terminus of the polyprotein to attach the construct to gold-coated surfaces. Importantly, force in a polyprotein propagates from the N to C terminus of each CnaB-TED repeat, which is not the physiological force pathway (*in vivo*, force propagates from the C terminus of CnaB to the point of ligand attachment at Gln-575; Fig. 6A).

Force-extension stretching of poly-CnaB_{D595A} TED produces sawtooth patterns with force peaks at repetitive intervals, characteristic of polyprotein mechanical unfolding (Fig. 2A). Strikingly, two populations of unfolding peaks are evident, a population of high-force peaks having unfolding forces of 258 ± 33 pN and a population of low-force peaks having unfolding forces of 105 ± 15 pN (Fig. 2B). Moreover, each high-force peak is often followed by one low-force peak.

Matched to structural data, the contour length increments following each unfolding peak can inform on the piecewise extension of the polyprotein (Fig. 1D). Unfolding extensions can be predicted by multiplying the number of extensible resi-

Mechanochemistry of a thioester bond in a bacterial adhesin

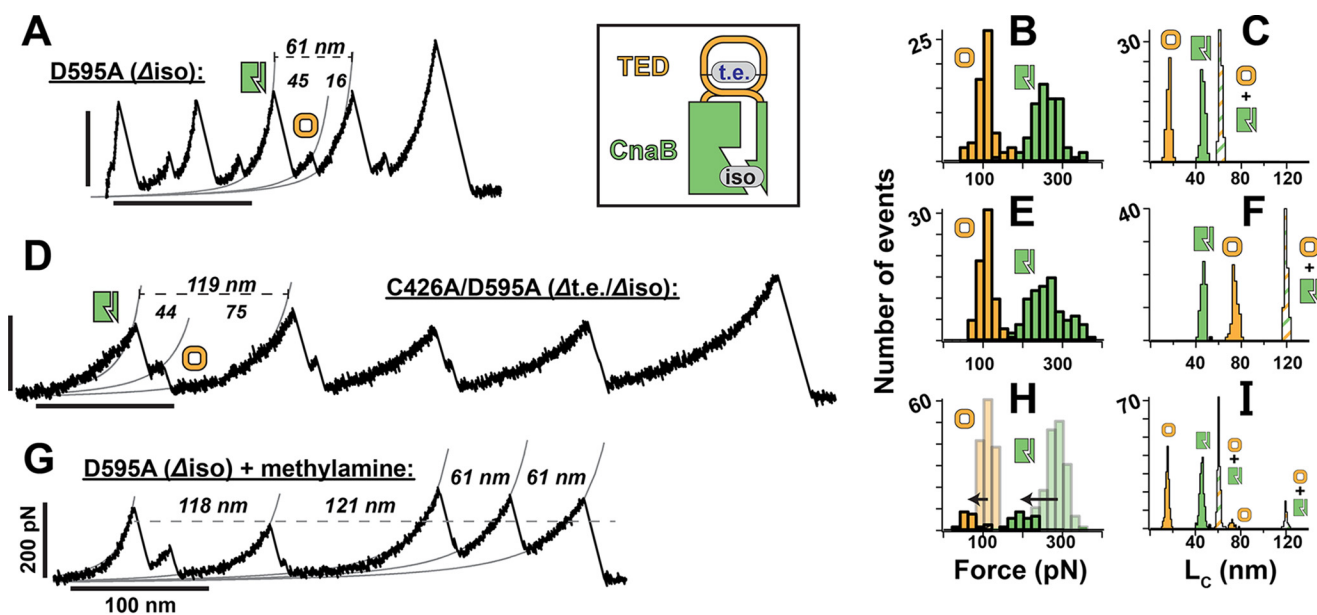


Figure 2. Spy0125 thioester bond can be discriminated by force spectroscopy. Force-extension recordings of the poly-CnaB_{D595A} TED (D595A (Δiso)) construct alone (A), supplemented with 500 mM methylamine (G), or of the thioester mutant poly-CnaB_{C426A/D595A} TED (C426A/D595A (Δt.e./Δiso)) construct (D). Force-extension recordings show four repetitive CnaB-TED unfolding events, each having a high force peak of CnaB unfolding (green squares) followed by a low force peak of TED unfolding (yellow circles). Contour length increments of worm-like chain fits are overlaid. Inset shows schematic contact map of CnaB-TED with isopeptide (iso) and thioester (t.e.) bonds, as in Fig. 1. Histograms of the peak unfolding force of CnaB and TED in the D595A construct alone (B, $n = 130$), with 500 mM methylamine (H, $n = 384$), or in the C426A/D595A construct (E, $n = 148$). H, unfolding forces from thioester-cleaved domains (~119 nm total extension) are shown in the foreground. Histograms of the peak-to-peak contour length increment (L_c) upon unfolding of TED, CnaB, or CnaB-TED combined in the D595A construct alone (C), with 500 mM methylamine (I), or in the C426A/D595A construct (F).

dues by 0.4 nm/residue (19), to give the extended length, and then subtracting the initial folded length. For CnaB-TED, we predict an unfolding extension of 119 nm (Table 1). However, an internal thioester bond could protect those residues sequestered behind the bond from mechanical unfolding, similar to the action of internal disulfide and isopeptide bonds (16, 19). Consequently, the predicted extension is proportionately reduced by the number of residues sequestered behind the bond. For CnaB-TED with a thioester bond, we predict an unfolding extension of 61 nm (Table 1). Peak-to-peak worm-like chain fits of the high-force unfolding events yield a reproducible contour length increment of 61.7 ± 1.4 nm (Fig. 2C). Notably, ~119 nm events were not observed in poly-CnaB_{D595A} TED force extension at pH 7.2 ($n = 68$), indicating that the thioester bond is 100% formed.

To further verify that the thioester bond is present, we removed the bond by mutating the participating cysteine (Cys-426) in a second polyprotein construct, poly-CnaB_{C426A/D595A} TED. In force-extension recordings on the thioester knock-out mutant, a new population of 119.4 ± 1.5 nm contour length increments between high-force peaks replaces the ~62 nm population, consistent with the predicted full extension of all 307 residues in CnaB-TED (Fig. 2, D and F). Meanwhile, the mechanical stability of the thioester knock-out is relatively unaffected, with the high-force peak unfolding at 254 ± 46 pN and the low-force peak unfolding at 106 ± 17 pN (Fig. 2E).

The staggered pattern of high-force peaks followed by low-force peaks is uncommon among polyprotein pulling experiments. We hypothesized that the low-force peak could originate in the discrete unfolding of the inserted TED, which would

only be exposed to force after the host CnaB had unfolded. Furthermore, we predicted that a mechanical clamp in the TED might consist of a set of six anti-parallel β -sheets beginning at Ala-393 and terminating at Gly-579, immediately following the thioester bond (supplemental Fig. S2). Full extension of the inserted TED would yield an unfolding length increment of 73 nm in the absence of the thioester bond and an increment of 15 nm in its presence (Table 1). As predicted, measurements of the extension following each low-force peak produce populations of 16.3 ± 1.9 nm contour length increments when the thioester bond is present and 74.3 ± 2.5 nm in the C426A thioester knock-out (Fig. 2, C and F). Moreover, independent unfolding of the host CnaB up to the proposed Ala-393–Gly-579 mechanical clamp would yield a predicted length increment of 46 nm (Table 1). Length increments between the high-force and low-force peaks measure ~46 nm in both polyprotein constructs, unaffected by the C426A mutation.

Thus, CnaB and TED unfold in two discrete steps: host CnaB unfolding occurs first at forces of ~255 pN with an ~46-nm extension, whereas the inserted TED unfolding follows and occurs at forces of ~105 pN with ~16- or ~74-nm extensions, depending on the presence or absence of the thioester bond. This reverse unfolding hierarchy, where a mechanically stable domain unfolds before a mechanically weaker domain, has been engineered previously by inserting the weaker fold of T4 lysozyme into a protein GB1 scaffold as a means of mechanically protecting the enzyme (22). The CnaB-TED host-insert pair is a natural occurrence of this mechanical protection strategy, as the CnaB protects the critical adhesin domain and its thioester bond. Moreover, autocatalytic formation of the Lys-297–Asp-595 isopeptide bond in the native Spy0125 renders

Table 1
Predicted and experimental unfolding contour lengths

The estimated unfolding (Est. unfold) and experimental unfolding (AFM unfold) extensions are given for CnaB and TED, alone or in combination, and with or without the thioester bond (T.E.). The number of residues in each domain is given, along with the boundary residues of each domain (No. of residues; see supplemental Fig. S2). Similarly, the number of residues protected behind the thioester bond or TED mechanical clamp is given (No. protected). Estimated unfolding extensions are calculated by multiplying the number of extensible residues (number of residues – number protected) by $0.4 \text{ nm}\cdot\text{residue}^{-1}$ (19) and subtracting the initial length, which is 3.5 nm for CnaB domains and 1.1 nm for TED alone (supplemental Fig. S2). When the thioester bond is present, 1 nm is added based on the estimated extended length of an internal isopeptide bond (16). In CnaB_{D595A} alone, 1.1 nm is added for the measured length of the TED mechanical clamp between Ala-393 and Gly-579 (supplemental Fig. S2).

Domains(s)	No. of residues	No. protected	T.E.	Est. unfold	AFM unfold
CnaB _{D595A} TED	307 (Thr-290–Lys-597)	149 (Cys-426–Gln-575)	Yes	^{nm} 60.7	61.7 ± 1.4 nm (<i>n</i> = 68)
CnaB _{C426A/D595A} TED	307 (Thr-290–Lys-597)		No	119.3m	119.4 ± 1.5 nm (<i>n</i> = 79)
TED	186 (Ala-393–Gly-579)	149 (Cys-426–Gln-575)	Yes	14.7	16.3 ± 1.9 nm (<i>n</i> = 62)
TED _{C426A}	186 (Ala-393–Gly-579)		No	73.3	74.3 ± 2.5 nm (<i>n</i> = 69)
CnaB _{D595A}	307 (Thr-290–Lys-597)	186 (Ala-393–Gly-579)		46.0	45.8 ± 2.1 nm (<i>n</i> = 62)

both the host CnaB and its inserted TED completely inextensible (supplemental Fig. S1, C and D).

Chemical cleavage of the thioester bond in a folded bacterial TED

The discrimination in unfolding contour length increment between the ~62-nm events of the poly-CnaB_{D595A}TED construct and the ~119-nm events of the poly-CnaB_{C426A/D595A}TED construct provides a robust single molecule assay for the presence or absence of the thioester bond. We therefore asked whether the thioester bond could be removed by chemical cleavage, rather than mutagenesis. We stretched the poly-CnaB_{D595A}TED construct in the presence of methylamine, a small molecule nucleophile commonly used in studies of the immune complement and bacterial thioesters (10, 23). The resultant force–extension recordings revealed a mixture of short “thioester-formed” extensions (61 nm) and long “thioester-cleaved” extensions (118 and 121 nm; Fig. 2G).

There are two noteworthy features of the trace in Fig. 2G. First, the long thioester-cleaved events match the unfolding patterns of the C426A mutant construct, with a CnaB extension of ~45 nm followed by a TED extension of ~72 nm (Fig. 2I). This full-length TED extension is consistent with a thioester bond that is chemically cleaved prior to mechanical unfolding. We considered an alternative scenario of “mechanically cryptic cleavage” analogous to the proteolytic gating of thioester reactivity in C3, C4, and A2M (4–8). In this scenario, nucleophilic attack would occur after mechanical unfolding and exposure of the previously buried thioester bond. This reaction mechanism has been well described for disulfide bond mechanochemistry, wherein an additional population of contour lengths is observed that follows only after domain unfolding and in the presence of a reducing agent (19). With CnaB–TED, cryptic cleavage is predicted to produce a new population with 58.6-nm extensions (supplemental Fig. S2). Instead, we observe populations of ~45- and ~72-nm extensions for chemical thioester cleavage that match those observed for C426A thioester mutagenesis, supporting a model of non-cryptic chemical cleavage.

Second, the first two thioester-cleaved domains in Fig. 2G unfold at lower forces than the latter two thioester-formed domains. With 500 mM methylamine (pH 7.2), thioester-cleaved domains account for 17% of total events (*n* = 210) and show CnaB unfolding at a weaker force of 198 ± 31 pN, compared with the 283 ± 25 pN unfolding forces of thioester-formed CnaB domains in the same traces (Fig. 2H). Thioester-

cleaved TED also unfolds at a weaker force (59 ± 16 pN) than the thioester-formed TED (109 ± 20 pN). This mechanical weakening only occurs with methylamine-mediated cleavage, as mutagenesis of the thioester bond does not appreciably affect stability (Fig. 2E; CnaB, 254 ± 46 pN; TED, 106 ± 17 pN). Methylamine substitution on the thioester bond produces *N*-methylglutamine, adding a methyl group into the protein-active site and potentially causing a steric destabilization in the structure. Similar mechanical weakening from the glutathionylation of buried cysteine residues has recently been reported (15). Notably, methylamine cleavage has a destabilizing effect on the thioester domain and a long-range destabilizing effect on the host CnaB domain (the CnaB mechanical clamp is ~25 Å from the thioester bond). As the destabilization of both the CnaB and TED is apparent at the point of mechanical unfolding, chemical cleavage must have occurred prior to unfolding. Thus, cleavage can occur via a non-cryptic methylamine attack on the folded protein, consistent with the observations of cleavage-dependent mechanical weakening and the ~72-nm force–extension contours.

Thioester cleavage is pH-dependent

As bacterial pili are subject to large shearing forces when adhering to host, we asked how mechanical unfolding would alter thioester reactivity. We did not observe the hypothesized 58.6-nm extension of mechanically cryptic thioester cleavage in our force extension assay. However, reaction kinetics depend on both time and force (24); in force extension, force is time-dependent. To measure force-dependent rates, we turned to force-clamp force spectroscopy, wherein the force on the molecule is held at a constant setpoint (24, 25). On a 90 pN force-clamp, CnaB domains unfold in ~38-nm steps, and TED domains unfold as either ~13-nm (thioester-formed) or ~63-nm (thioester-cleaved) steps (supplemental Fig. S3, B and D). The weaker TED unfolds rapidly after CnaB unfolding such that the two steps may appear as a single step, especially at forces of >90 pN (supplemental Fig. S3, A and C). Moreover, as methylamine cleavage weakens CnaB–TED, thioester-cleaved events occur more rapidly at low forces, thereby biasing the observation toward cleavage. Therefore, in all subsequent work, we applied a linearly increasing force setpoint, termed force-ramp, to resolve both low-force and high-force events without bias (Fig. 3) (15).

On a $100 \text{ pN}\cdot\text{s}^{-1}$ force-ramp, thioester-formed domains unfold in a combined CnaB–TED step of 54.9 ± 1.2 -nm incre-

Mechanochemistry of a thioester bond in a bacterial adhesin

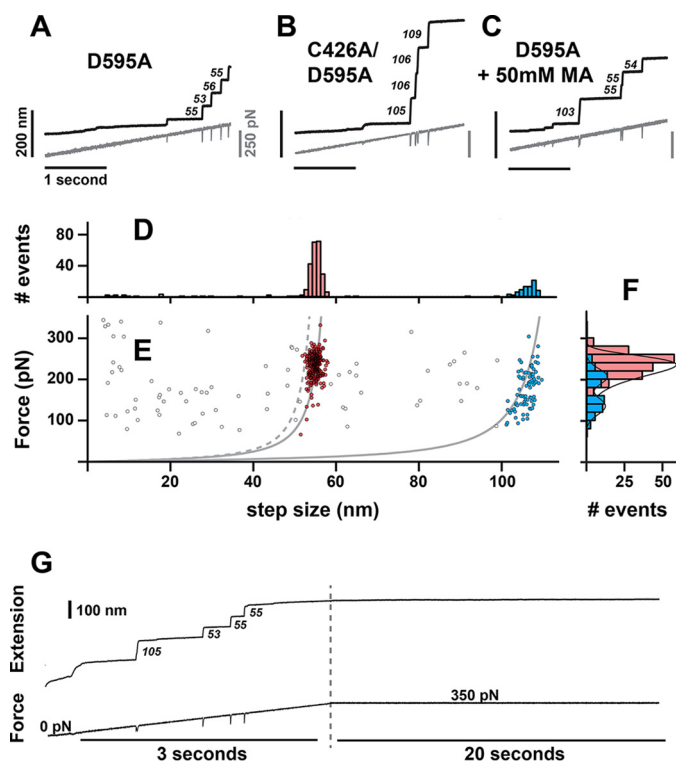


Figure 3. Nucleophilic cleavage of the Spy0125 thioester bond. Force-ramp recordings of the poly-CnaB_{D595A}TED (D595A) construct alone (A), in the presence of 50 mM methylamine (C), or of the thioester mutant poly-CnaB_{C426A/D595A}TED (C426A/D595A) construct (B). Step sizes (in nanometers) are indicated. The linearly increasing force is shown in gray below each trace. D, step size; F, unfolding force histograms of the D595A construct in the presence of 50 mM methylamine at pH 8.5. E, all individual events ($n = 398$) are overlaid on the experimental worm-like chain contours for thioester-formed ($L_C = 61.7$ nm) and thioester-cleaved ($L_C = 119.4$ nm) unfolding, and on the predicted worm-like chain contour for cryptic thioester cleavage (dotted line, $L_C = 58.6$ nm). Events falling within three standard deviations of the step size centroids are marked in red for thioester-formed (54.9 ± 1.2 nm) and blue for thioester-cleaved (106.5 ± 1.8 nm). The single thioester-formed unfolding force population (in red, $n = 199$) is fit with the distribution of Schlierf *et al.* (26) with an $\alpha_0 = 0.8 \cdot 10^{-4} \text{ s}^{-1}$ and a $\Delta x = 0.16$ nm. The two thioester-cleaved populations are fit with a double Gaussian function (in blue, $n = 69$). G, ramp-clamp recording of poly-CnaB_{D595A}TED wherein all domains are unfolded on an initial force ramp to 350 pN, after which force is clamped at a constant value of 350 pN. The initial ramp shows one thioester-cleaved (105 nm) and three thioester-formed (53–55 nm) unfolding steps.

ments, with unfolding forces of ~ 236 pN that follow a standard distribution for mechanical unfolding across a single energy barrier (Fig. 3, D and F), as described by Schlierf *et al.* (26). Thioester-cleaved domains unfold in 106.5 ± 1.8 -nm increments as two mechanically distinct populations at weaker forces of 136 ± 21 and 207 ± 19 pN. These ~ 55 - and ~ 107 -nm steps track with the worm-like chain contours for the 61.7- and 119.4-nm extensions, respectively (Fig. 3E).

The fraction of thioester-cleaved events is heavily pH-dependent, ranging between 1% at pH 7.2, 26% at pH 8.5, and 80% at pH 10, in reactions with 50 mM methylamine (Fig. 4B and supplemental Fig. S4). Higher pH likely favors the forward reaction by deprotonating methylamine and increasing its nucleophilic character. In contrast, 99% of domains have a formed thioester bond at pH 10 in the absence of methylamine (Fig. 4A).

Although methylamine is present physiologically as a metabolic end product (27), we asked whether a larger biologically

relevant amine, histamine, would exhibit nucleophilic attack on the bacterial thioester. In the presence of 50 mM histamine at pH 8.5, thioester cleavage plateaus at 20%, comparable with the activity of methylamine (supplemental Fig. S5).

Thioester cleavage is not observed after mechanical unfolding

We predicted four signature observations of mechanically cryptic thioester cleavage based on precedent from single-molecule studies of cryptic disulfide bond reduction (24, 28) as follows: 1) the appearance of a new population of step sizes resulting from cryptic cleavage; 2) 2-fold increase in the total number of steps observed when nucleophile is present (the second set of steps resulting from cryptic cleavage); 3) rate of cryptic cleavage that varies with reaction conditions; and 4) secondary kinetic regime for cryptic cleavage that is separate from unfolding.

We do not observe cryptic thioester cleavage consistent with any of these four predictions. First, the identical ~ 55 -nm thioester-formed steps are observed in all reaction conditions (pH 7.2–10; 0 and 50 mM methylamine) without the appearance of a shorter step size population (Fig. 3E and supplemental Fig. S6). In contrast, the population of ~ 107 -nm steps from non-cryptic thioester cleavage increases with pH and methylamine concentration. Second, there is no observed increase in the total number of steps that occurs with more stringent reaction conditions (supplemental Table S1).

Finally, we sought to capture any cryptic thioester cleavage occurring on a secondary kinetic regime after mechanical unfolding. Herein, we implemented a two-part “ramp-clamp” protocol, combining a short force-ramp to unfold and resolve the thioester state of each domain and a force-clamp to monitor subsequent cleavage events at a fixed force. The ramp-clamp protocol thereby segregates domain unfolding steps from thioester cleavage steps. For example, in the ramp-clamp recording in Fig. 3G, three domains with formed thioester bonds unfold on the initial force-ramp; however, no additional steps are observed during the subsequent 20 s of force-clamp observation at 350 pN. As force can affect the rate of chemical reactions, we explored a range of forces from 50 to 350 pN. In 30 thioester-minutes of observation on force-clamp, a total of 7 short steps of 4–32 nm were observed during the force-clamp. No steps have been observed within the 44.6–53.5-nm range predicted for thioester cleavage at these forces (supplemental Table S2). The absence of cryptic cleavage steps after CnaB-TED unfolding might suggest that mechanical unfolding inhibits thioester reactivity, which we otherwise readily observe in folded domains. However, we caution against this conclusion due to two limitations of the single molecule thioester assay. First, thioester reactivity may be sharply force-dependent and may occur at forces < 50 pN that are difficult to access with AFM-based single-molecule force spectroscopy. Alternative force spectroscopy techniques that are better suited for low-force measurement, such as magnetic tweezers (29), may resolve thioester reactivity in the regime < 50 pN. Second, and more significantly, the apparent absence of cryptic thioester cleavage in force-extension or ramp-clamp experiments leaves us without a single-molecule fingerprint for such events. The predicted contour length from cryptic cleavage, 58.6 nm (sup-

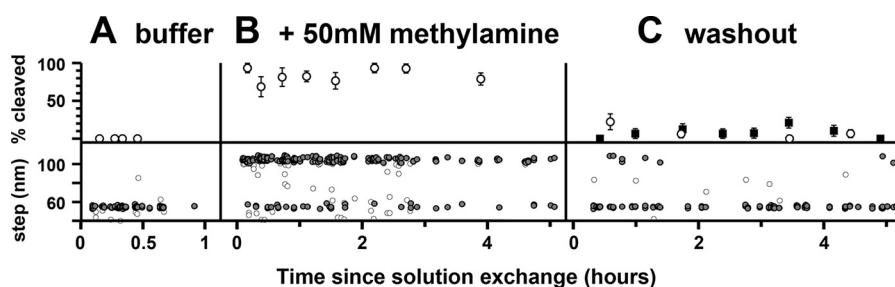


Figure 4. Spy0125 thioester bond spontaneously reforms. At bottom, step size measurements from force-ramp recordings of the D595A construct from prior to (A, buffer, $n = 105$), upon addition of methylamine (B, +50 mM methylamine, $n = 450$), and after rinsing away the methylamine (C, washout, $n = 192$). Filled circles indicate events falling within three standard deviations of the step size centroids for thioester-formed (54.9 ± 1.2 nm) or thioester-cleaved (106.5 ± 1.8 nm) that were considered in subsequent analysis. All recordings were carried out in borax-buffered saline at pH 10. At top, binned averages of the percent of thioester-cleaved domains at pH 10 (open circles, bin size = 5–8 recordings). Washout into borax-buffered saline at pH 8.5 shows comparable thioester reformation (closed squares, bin size = 7 recordings). Error bars indicate standard errors of the mean.

plemental Fig. S2), is comparable with the experimentally measured contour length of combined CnaB-TED unfolding, 61.7 nm (Fig. 3E). At 200 pN, CnaB and TED events, which are otherwise discrete, merge into a single unfolding step of 54.0 ± 1.1 nm (supplemental Fig. S3E). Cryptic cleavage at 200 pN would yield a predicted step of 51.9 nm. The absence of the hypothesized cryptic cleavage populations in force extension and in 30 min of force-clamp observation suggests that thioester reactivity is inhibited by mechanical unfolding. However, lacking a defined fingerprint for cryptic cleavage, we cannot definitively exclude this cryptic cleavage event.

Thioester bond reversibly reforms after nucleophile washout

We sought to apply our single molecule thioester assay to measure the noncryptic reaction kinetics in the folded protein. In their discovery of the first bacterial TED, Pointon *et al.* (10) applied a colorimetric reporter to monitor CnaB-TED thioester cleavage in solution, reporting that the reaction with methylamine plateaus within the first 400 s at pH 7.5 and with 6 M urea. We measured the fraction of thioester-cleaved events as a function of time after methylamine addition (Fig. 4). Kinetic measurements in our force spectroscopy assay are limited by the time delay in finding single molecules, with the earliest recording made 4 min after solution exchange. The fractional thioester cleavage already plateaus by the first aggregated time points at 7.5–10 min (Fig. 4B and supplemental Fig. S4B), consistent with these earlier studies of CnaB-TED reactivity in bulk. We subsequently washed away the methylamine nucleophile from the AFM fluid chamber with excess buffer, and we asked whether the cleaved thioester bonds could spontaneously reform. In the presence of methylamine at pH 10, 80% of domains exhibit chemical cleavage, with only 20% of events retaining the formed bond. After washout, up to 94% of domains have the formed thioester bond (Fig. 4C). Critically, the step sizes before methylamine addition and after methylamine removal are identical, indicating that the same Cys-426–Gln-575 bond is again present. This back reaction proceeds rapidly, reaching completion by the first aggregated time point at 26 min. This recovery of the shorter thioester-formed unfolding steps is likely the result of autocatalytic thioester bond reformation, which proceeds with a half-life of <7 min (as estimated from the recovery from a baseline cleavage fraction of 80 to 6% in 26 min).

Similarly, we followed experiments with 50 mM histamine, which cleaves the thioester bond comparable with methylamine (20% cleavage at pH 8.5), with a rinse to remove the attacking nucleophile. Again, the step sizes return to the shorter thioester-formed length after washout (4% cleavage; supplemental Fig. S5). Thus, for both soluble nucleophiles methylamine and histamine, cleavage of the thioester exists in equilibrium with bond reformation.

Discussion

In their initial work on the bacterial thioester performed in bulk solution studies, Pointon *et al.* (10) observed that the reaction with methylamine plateaued before reaching completion. The authors postulated that the remainder of CnaB-TED was unreactive as it lacked formed thioester bonds. Here, applying a single molecule assay to discriminate the thioester state, we find that 100% of the CnaB-TED domains contain the formed Cys-Gln bond at neutral pH and in the absence of nucleophile (Fig. 2C). Moreover, a chemically cleaved thioester bond spontaneously reforms, which becomes evident after the nucleophile is removed (Fig. 4C). Thus, we can propose an alternative explanation for the incomplete forward reaction: the nucleophilic attack on the thioester exists in equilibrium with reformation of the bond. The forward reaction between methylamine and the Cys-Gln thioester yields *N*-methylglutamine and the thiolate anion of cysteine. This free thiolate could attack the glutamyl carbonyl in a reverse substitution reaction to reform the thioester bond (Fig. 5, A–C). Precedent for this mechanism can be found in biochemical studies on the C3 immune complement protein. C3 harbors an internal thioester bond, formed between cysteine and glutamine residues at positions i and $i + 3$. In the classical complement activation pathway, the C3 thioester bond is cryptic within a hydrophobic core, exposed to irreversibly react with ligand only after proteolytic cleavage of C3. However, a small fraction of C3, as much as 1% in certain disease states, can activate in the absence of proteolysis (30). In this so-called “tick-over” mechanism, water and small amine nucleophiles, including methylamine, can cleave the buried thioester bond in the native C3 structure. Following cleavage, the thioester bond can spontaneously reform with release of the nucleophile, or C3 can undergo a large structural rearrangement after which the reaction is irreversible (31). With ammonia as the substituting nucleophile, C3 thioester reformation

Mechanochemistry of a thioester bond in a bacterial adhesin

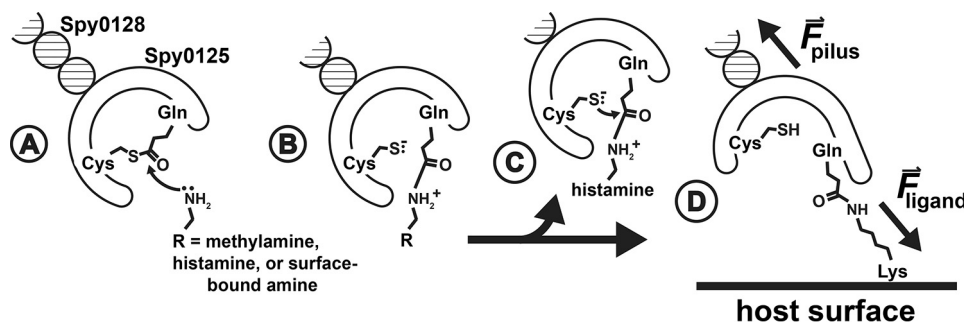


Figure 5. Mechanism for reversible force-dependent binding in a thioester-containing adhesin. *A*, amine nucleophile is able to attack the thioester bond in a folded Spy0125 adhesin. *B*, amine nucleophile substitutes out the cysteine thiol and forms an intermolecular isopeptide bond. *C*, in the reverse substitution reaction, the free thiolate ion attacks at the glutamyl carbonyl, reforming the thioester and breaking the adhesin-ligand bond. The reverse reaction proceeds rapidly when the ligand does not exert force across the bond, as would soluble nucleophiles such as methylamine or histamine. *D*, however, force applied through a surface-associated ligand, such as a lysine in the extracellular matrix, can displace the glutamine and cysteine residues relative to one another, likely disfavoring thioester reformation and establishing a stable covalent bond with ligand.

occurs with a half-life of 1.5 h (23). In contrast, we measure thioester reformation in the bacterial TED with a half-life of under a few minutes.

The apparent inhibition of thioester reactivity after mechanical unfolding also follows a precedent established in the study of C3 activity. After proteolytic cleavage, the exposed C3 thioester irreversibly reacts with a half-life on the order of microseconds (8). By contrast, a synthetic peptide analog of the C3 thioester bond hydrolyzes at a relatively slow rate, with a half-life of 10 h (32). This sharp discrepancy in reaction rates may result from the contribution of other active-site residues in the native C3, including critical His-1104 and Glu-1106 residues (33), that are absent in the synthetic peptide.

Indeed, mechanical force may alter the thioester active site in the CnaB-TED domains of Spy0125 and thereby alter reactivity. *In vivo*, CnaB-TED is pulled from the pilus tether at its C terminus, and from the point of ligand attachment at the thioester's glutamyl-carbonyl of Gln-575, rather than from the N and C termini as applied in our experiments (Fig. 6A). As we could not experimentally access the physiological pulling axis, we simulated how force exerted by a ligand might alter the thioester active site. Force propagates from the point of ligand substitution at Gln-575 to the C terminus (Thr-603; Fig. 6B, pathway highlighted in red), leaving the tertiary structures of CnaB and TED largely unperturbed. Gln-575 is explicitly under force and elongates along the pulling axis. However, most active-site residues fall outside of the force propagation pathway, including Gln-512 and Tyr-516 of a conserved TQXA(I/V)W motif (11), and are not affected by the pulling simulation (Fig. 6C). Notably, this Tyr-516 residue is at a conserved position that is required for nucleophilic cleavage of the thioester bond (9). As mechanical force exerted by ligand dislodges Gln-575 from the thioester active site, this force vector might also inhibit thioester reformation. We have observed non-cryptic cleavage of the thioester bond with methylamine and histamine nucleophiles and reversible thioester reformation at zero force. Soluble ligands do not exert a vectorial force, and dissociate from the bacterial TED as the freed thiolate ion can substitute out the ligand and reform the bond (Fig. 5, B and C). Histamine is stored in mast cell granules at ~30–90 mM (34) and is released at sites of injury and inflammation where it is likely

to encounter invading bacteria. Consequently, histamine may act as a suicide substrate against thioester adhesins; however, it could only have a transient inhibitory effect due to spontaneous thioester reformation, during which time histamine is rapidly degraded by extracellular methyltransferases (35).

By contrast, a surface-associated ligand, such as the lysine of an extracellular matrix component, might displace the glutamyl-carbonyl from the thioester active site and disfavor the reverse reaction (Figs. 5D and 6B). As such, a surface-associated ligand under sufficient force may cross-link the thioester adhesin with a longer lifetime. Force-activated binding mechanisms have been well characterized for Gram-negative bacteria, most notably for the “catch-bond” of the *Escherichia coli* pilus adhesin (36, 37). Force-activated adhesion has been observed in cellular assays with two Gram-positive species, *Staphylococcus aureus* and *Streptococcus gordonii* (38, 39), although the underlying molecular mechanisms are poorly understood. We speculate that the thioester adhesin may afford this molecular switch between reversible reactivity at zero force and irreversible covalent binding at sufficiently high force.

Experimental procedures

Protein engineering and purification

The *S. pyogenes spy0125* gene on a pOPIN-F plasmid was generously provided by Mark Banfield (John Innes Centre, Norwich, UK). An internal BglII restriction site was removed via overlap extension PCR using the following primers: 5'-GTCTATTGCTTTAATGCAGACCTAAAATCTCCACCAGAC-3' (forward) and 5'-GTCTGGTGGAGATTTAGGTCTGCATTAAAGCAATAGAC-3' (reverse). To assemble the DNA for the polyprotein constructs, we PCR-amplified from the *spy0125* gene using a forward primer with a flanking BamHI restriction site (5'-CTAGGATCCAATCAACCTCAAACGACTTC-3') and a reverse primer with flanking BglII and KpnI restriction sites (5'-GTCCGTACCTTAGCAACAAGATCTAACTTCTTTTGTAGCTTCCATAC-3'). The reverse primer also carried the D595A point mutation (underlined in the reverse primer), and two terminal cysteine residues. The C426A mutation was introduced via overlap extension PCR using the following primers: 5'-GGAAGTTCACAGGTT-

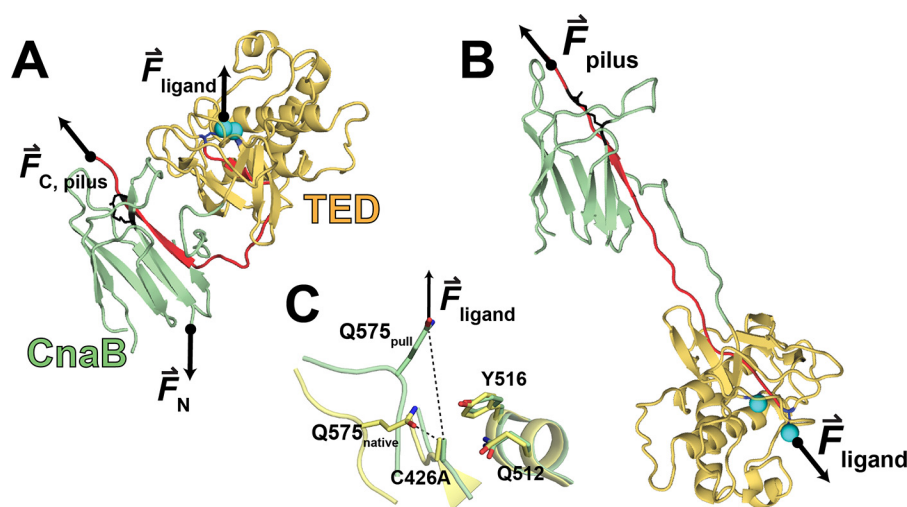


Figure 6. Physiological pulling axis in Spy0125. Structure of the CnaB-TED domains at the beginning (A) and after 300 ps (B) in a steered molecular dynamics simulation with pulling from the C_δ of the Gln-575 carbonyl. A crystal structure with the C426A mutation was used (PDB code 4bug) to mimic nucleophilic cleavage by ligand. The experimental pulling axis (F_N and F_C) and the physiological pulling axis (F_{pilus} and F_{ligand}) are shown, with the native force propagation pathway indicated in red. The thioester residues Gln-575 and C426A are represented with blue spheres. C, overlay of the thioester active site at the beginning (in yellow) and at the end (in green) of the simulated pull.

GTCTATGCCTTTAATGCAGACCTAAAATC-3' (forward) and 5'-GATTTTAGGTCTGCATTAAAGGCATAGACAACCTGTGAACTTCC-' (reverse). The C426A mutagenesis primers also contain the silent mutation removing the internal BglII restriction site, introduced previously. Both the poly-CnaB_{D595A}-TED and poly-CnaB_{C426A/D595A}-TED polyproteins were assembled using multistep cloning with the BamHI, BglII, and KpnI restriction sites, as described previously (40). In the final step, the polyprotein genes were transferred to a pQE80L (Qiagen) expression vector carrying an N-terminal His₆ tag.

Polyproteins were expressed and purified as described previously (21). Briefly, *E. coli* ERL cells were transformed with the polyprotein expression plasmids, induced with 1 mM isopropyl β-D-1-thiogalactopyranoside, overnight at 25 °C, and then lysed by French press. Two-step protein purification was performed with an initial Ni²⁺-nitrilotriacetic acid His GraviTrap affinity column (GE Healthcare), followed by a gel filtration step in a Superdex 200 FPLC column (GE Healthcare) in 10 mM Hepes (pH 7.2), 150 mM NaCl, 1 mM EDTA. Purified proteins could be stored at 4 °C for up to 2 months.

Single-molecule AFM

For single-molecule AFM experiments, we deposited ~20 μl of polyprotein from the FPLC purification peak (typically ~1 μM) onto freshly evaporated gold coverslips. AFM experiments were performed on a custom-built setup (41) using Bruker Model MLCT cantilevers (Bruker AFM Probes, Camarillo, CA). Cantilevers were calibrated using the equipartition theorem (42) and had spring constants of 10–20 pN·nm⁻¹. To acquire individual molecules, the cantilever was first approached to the surface to a contact force of 1500–2000 pN and then retracted to measure protein mechanics under a pulling force. In force-extension experiments, the retraction velocity was a constant 400 nm·s⁻¹. In force-ramp experiments, the retraction was performed by applying a linearly increasing pulling load at a rate of 100 pN·s⁻¹. In both force-ramp and force-clamp experiments, the force on the cantilever was held con-

stant through a proportional, integral, and differential feedback (25). Buffered solutions with methylamine hydrochloride (Sigma) or histamine (Sigma) were prepared at pH 7.2 with 10 mM Hepes, 150 mM NaCl, and 1 mM EDTA, whereas the buffered solutions were prepared at pH 8.5 and pH 10 with 50 mM borax, 150 mM NaCl, and 1 mM EDTA. In washout experiments, the AFM fluid chamber (~60 μl volume) was rinsed with >1 ml of buffer without nucleophile.

Data analysis

All AFM force spectroscopy data were analyzed with custom-written software in IgorPro (WaveMetrics). Only recordings having a pre-defined fingerprint with 2–4 sequential CnaB-TED unfolding events were included for data analysis. Furthermore, we excluded force-ramp recordings that detached below 300 pN on the force ramp. This exclusion criteria was introduced to prevent a bias toward observing thioester-cleaved domains, which unfold at weaker forces and are therefore more likely to be observed in recordings where detachment occurs early. Force-extension recordings were fit with the worm-like chain model of polymer elasticity (43) to measure contour length increments. Unless otherwise noted, histograms were fit with Gaussian distributions, with the centroid and standard deviation of the Gaussian fit reported. For nucleophile cleavage and reformation assays, unfolding steps within 3 standard deviations of each centroid, 54.9 ± 1.2 nm for thioester-formed and 106.5 ± 1.8 nm for thioester-cleaved domains, were considered.

SMD simulations

Steered molecular dynamics simulations (Fig. 6) were performed on the crystal structure Spy0125 C426A (PDB code 4bug) with the GROMACS 5.1.2 package, using the OPLS-AA/L all-atom force field. The system was energy-minimized and equilibrated in constant volume and constant pressure ensembles. Pulling simulations were carried out with a pulling rate of 0.03 nm·ps⁻¹ along the physiological axis from C_δ of

Mechanochemistry of a thioester bond in a bacterial adhesin

Gln-575 to the C terminus. Additional detail on the simulation procedure can be found in [supplemental material](#).

Author contributions—D. J. E. and J. M. F. designed the research; D. J. E. and A. Q. L. performed the experiments and analyzed the data; and D. J. E. and J. M. F. wrote the paper.

Acknowledgments—We thank Mark Banfield (John Innes Centre, Norwich, United Kingdom) for generously providing the spy0125 gene. *E. coli* ERL cells were a gift from Robert T. Sauer (Massachusetts Institute of Technology, Cambridge, MA).

References

- Scheffner, M., Nuber, U., and Hübregtse, J. M. (1995) Protein ubiquitination involving an e1-e2-e3 enzyme ubiquitin thioester cascade. *Nature* **373**, 81–83
- Bhaumik, P., Koski, M. K., Glumoff, T., Hiltunen, J. K., and Wierenga, R. K. (2005) Structural biology of the thioester-dependent degradation and synthesis of fatty acids. *Curr. Opin. Struct. Biol.* **15**, 621–628
- Mitchell, C. A., Shi, C., Aldrich, C. C., and Gulick, A. M. (2012) Structure of pa1221, a nonribosomal peptide synthetase containing adenylation and peptidyl carrier protein domains. *Biochemistry* **51**, 3252–3263
- García-Ferrer, I., Arède, P., Gómez-Blanco, J., Luque, D., Duquerroy, S., Castón, J. R., Goulas, T., and Gomis-Rüth, F. X. (2015) Structural and functional insights into *Escherichia coli* $\alpha 2$ -macroglobulin endopeptidase snap-trap inhibition. *Proc. Natl. Acad. Sci. U.S.A.* **112**, 8290–8295
- Law, S. K., and Dodds, A. W. (1997) The internal thioester and the covalent binding properties of the complement proteins c3 and c4. *Protein Sci.* **6**, 263–274
- Wong, S. G., and Dessen, A. (2014) Structure of a bacterial $\alpha 2$ -macroglobulin reveals mimicry of eukaryotic innate immunity. *Nat. Commun.* **5**, 4917
- Dodds, A. W., Ren, X. D., Willis, A. C., and Law, S. K. (1996) The reaction mechanism of the internal thioester in the human complement component c4. *Nature* **379**, 177–179
- Sim, R. B., Twose, T. M., Paterson, D. S., and Sim, E. (1981) The covalent-binding reaction of complement component c3. *Biochem. J.* **193**, 115–127
- Linke-Winnebeck, C., Paterson, N. G., Young, P. G., Middleditch, M. J., Greenwood, D. R., Witte, G., and Baker, E. N. (2014) Structural model for covalent adhesion of the *Streptococcus pyogenes* pilus through a thioester bond. *J. Biol. Chem.* **289**, 177–189
- Pointon, J. A., Smith, W. D., Saalbach, G., Crow, A., Kehoe, M. A., and Banfield, M. J. (2010) A highly unusual thioester bond in a pilus adhesin is required for efficient host cell interaction. *J. Biol. Chem.* **285**, 33858–33866
- Walden, M., Edwards, J. M., Dziejulska, A. M., Bergmann, R., Saalbach, G., Kan, S. Y., Miller, O. K., Weckener, M., Jackson, R. J., Shirran, S. L., Botting, C. H., Florence, G. J., Rohde, M., Banfield, M. J., and Schwarz-Linek, U. (2015) An internal thioester in a pathogen surface protein mediates covalent host binding. *Elife* **4**, 10.7554/eLife.06638
- Rivas-Pardo, J. A., Eckels, E. C., Popa, I., Kosuri, P., Linke, W. A., and Fernández, J. M. (2016) Work done by titin protein folding assists muscle contraction. *Cell Rep.* **14**, 1339–1347
- Möller, J., Lühmann, T., Chabria, M., Hall, H., and Vogel, V. (2013) Macrophages lift off surface-bound bacteria using a filopodium-lamellipodium hook-and-shovel mechanism. *Sci. Rep.* **3**, 2884
- Johnson, C. P., Tang, H. Y., Carag, C., Speicher, D. W., and Discher, D. E. (2007) Forced unfolding of proteins within cells. *Science* **317**, 663–666
- Alegre-Cebollada, J., Kosuri, P., Giganti, D., Eckels, E., Rivas-Pardo, J. A., Hamdani, N., Warren, C. M., Solaro, R. J., Linke, W. A., and Fernández, J. M. (2014) S-Glutathionylation of cryptic cysteines enhances titin elasticity by blocking protein folding. *Cell* **156**, 1235–1246
- Echelman, D. J., Alegre-Cebollada, J., Badilla, C. L., Chang, C., Ton-That, H., and Fernández, J. M. (2016) CnaA domains in bacterial pili are efficient dissipaters of large mechanical shocks. *Proc. Natl. Acad. Sci. U.S.A.* **113**, 2490–2495
- Baker, E. N., Squire, C. J., and Young, P. G. (2015) Self-generated covalent cross-links in the cell-surface adhesins of Gram-positive bacteria. *Biochem. Soc. Trans.* **43**, 787–794
- Rearson-Robinson, M. E., and Ton-That, H. (2015) Disulfide-bond-forming pathways in Gram-positive bacteria. *J. Bacteriol.* **198**, 746–754
- Ainavarapu, S. R., Brujic, J., Huang, H. H., Wiita, A. P., Lu, H., Li, L., Walther, K. A., Carrion-Vazquez, M., Li, H., and Fernandez, J. M. (2007) Contour length and refolding rate of a small protein controlled by engineered disulfide bonds. *Biophys. J.* **92**, 225–233
- Smith, W. D., Pointon, J. A., Abbot, E., Kang, H. J., Baker, E. N., Hirst, B. H., Wilson, J. A., Banfield, M. J., and Kehoe, M. A. (2010) Roles of minor pilin subunits spy0125 and spy0130 in the serotype m1 *Streptococcus pyogenes* strain sf370. *J. Bacteriol.* **192**, 4651–4659
- Alegre-Cebollada, J., Badilla, C. L., and Fernández, J. M. (2010) Isopeptide bonds block the mechanical extension of pili in pathogenic *Streptococcus pyogenes*. *J. Biol. Chem.* **285**, 11235–11242
- Peng, Q., and Li, H. (2009) Domain insertion effectively regulates the mechanical unfolding hierarchy of elastomeric proteins: toward engineering multifunctional elastomeric proteins. *J. Am. Chem. Soc.* **131**, 14050–14056
- Pangburn, M. K. (1992) Spontaneous reformation of the intramolecular thioester in complement protein c3 and low temperature capture of a conformational intermediate capable of reformation. *J. Biol. Chem.* **267**, 8584–8590
- Wiita, A. P., Ainavarapu, S. R., Huang, H. H., and Fernandez, J. M. (2006) Force-dependent chemical kinetics of disulfide bond reduction observed with single-molecule techniques. *Proc. Natl. Acad. Sci. U.S.A.* **103**, 7222–7227
- Oberhauser, A. F., Hansma, P. K., Carrion-Vazquez, M., and Fernandez, J. M. (2001) Stepwise unfolding of titin under force-clamp atomic force microscopy. *Proc. Natl. Acad. Sci. U.S.A.* **98**, 468–472
- Schlierf, M., Li, H., and Fernandez, J. M. (2004) The unfolding kinetics of ubiquitin captured with single-molecule force-clamp techniques. *Proc. Natl. Acad. Sci. U.S.A.* **101**, 7299–7304
- Mitchell, S. C., and Zhang, A. Q. (2001) Methylamine in human urine. *Clin. Chim. Acta* **312**, 107–114
- Kahn, T. B., Fernández, J. M., and Perez-Jimenez, R. (2015) Monitoring oxidative folding of a single protein catalyzed by the disulfide oxidoreductase dsba. *J. Biol. Chem.* **290**, 14518–14527
- Popa, I., Rivas-Pardo, J. A., Eckels, E. C., Echelman, D. J., Badilla, C. L., Valle-Orero, J., and Fernández, J. M. (2016) A halotag anchored ruler for week-long studies of protein dynamics. *J. Am. Chem. Soc.* **138**, 10546–10553
- Nilsson, B., and Nilsson Ekdahl, K. (2012) The tick-over theory revisited: is c3 a contact-activated protein? *Immunobiology* **217**, 1106–1110
- Nishida, N., Walz, T., and Springer, T. A. (2006) Structural transitions of complement component c3 and its activation products. *Proc. Natl. Acad. Sci. U.S.A.* **103**, 19737–19742
- Khan, S. A., Sekulski, J. M., and Erickson, B. W. (1986) Peptide models of protein metastable binding sites: competitive kinetics of isomerization and hydrolysis. *Biochemistry* **25**, 5165–5171
- Janssen, B. J., Huizinga, E. G., Raaijmakers, H. C., Roos, A., Daha, M. R., Nilsson-Ekdahl, K., Nilsson, B., and Gros, P. (2005) Structures of complement component c3 provide insights into the function and evolution of immunity. *Nature* **437**, 505–511
- Prussin, C., and Metcalfe, D. D. (2003) IgE, mast cells, basophils, and eosinophils. *J. Allergy Clin. Immunol.* **111**, S486–S494
- Stone, K. D., Prussin, C., and Metcalfe, D. D. (2010) Ige, mast cells, basophils, and eosinophils. *J. Allergy Clin. Immunol.* **125**, S73–S80
- Schwartz, D. J., Kalas, V., Pinkner, J. S., Chen, S. L., Spaulding, C. N., Dodson, K. W., and Hultgren, S. J. (2013) Positively selected fimh residues enhance virulence during urinary tract infection by altering fimh conformation. *Proc. Natl. Acad. Sci. U.S.A.* **110**, 15530–15537
- Sauer, M. M., Jakob, R. P., Eras, J., Baday, S., Eriş, D., Navarra, G., Bernèche, S., Ernst, B., Maier, T., and Glockshuber, R. (2016) Catch-bond mechanism of the bacterial adhesin fimh. *Nat. Commun.* **7**, 10738
- George, N. P., Wei, Q., Shin, P. K., Konstantopoulos, K., and Ross, J. M. (2006) *Staphylococcus aureus* adhesion via spa, clfa, and sdrce to immo-

- bilized platelets demonstrates shear-dependent behavior. *Arterioscler. Thromb. Vasc. Biol.* **26**, 2394–2400
39. Ding, A. M., Palmer, R. J., Jr., Cisar, J. O., and Kolenbrander, P. E. (2010) Shear-enhanced oral microbial adhesion. *Appl. Environ. Microbiol.* **76**, 1294–1297
40. Carrion-Vazquez, M., Oberhauser, A. F., Fowler, S. B., Marszalek, P. E., Broedel, S. E., Clarke, J., and Fernandez, J. M. (1999) Mechanical and chemical unfolding of a single protein: a comparison. *Proc. Natl. Acad. Sci. U.S.A.* **96**, 3694–3699
41. Popa, I., Kosuri, P., Alegre-Cebollada, J., Garcia-Manyes, S., and Fernandez, J. M. (2013) Force dependency of biochemical reactions measured by single-molecule force-clamp spectroscopy. *Nat. Protoc.* **8**, 1261–1276
42. Florin, E. L., Rief, M., Lehmann, H., Ludwig, M., Dornmair, C., Moy, V. T., and Gaub, H. E. (1995) Sensing specific molecular interactions with the atomic force microscope. *Biosens. Bioelectron.* **10**, 895–901
43. Bustamante, C., Marko, J. F., Siggia, E. D., and Smith, S. (1994) Entropic elasticity of λ -phage DNA. *Science* **265**, 1599–1600

Mechanical forces regulate the reactivity of a thioester bond in a bacterial adhesin

Daniel J. Echelman, Alex Q. Lee and Julio M. Fernández

J. Biol. Chem. 2017, 292:8988-8997.

doi: 10.1074/jbc.M117.777466 originally published online March 27, 2017

Access the most updated version of this article at doi: [10.1074/jbc.M117.777466](https://doi.org/10.1074/jbc.M117.777466)

Alerts:

- [When this article is cited](#)
- [When a correction for this article is posted](#)

[Click here](#) to choose from all of JBC's e-mail alerts

Supplemental material:

<http://www.jbc.org/content/suppl/2017/03/27/M117.777466.DC1>

This article cites 43 references, 21 of which can be accessed free at <http://www.jbc.org/content/292/21/8988.full.html#ref-list-1>